Protein Science (1999), *8*:2010–2018. Cambridge University Press. Printed in the USA.

Pig heart short chain L-3-hydroxyacyl-CoA dehydrogenase revisited: Sequence analysis and crystal structure determination

JOSEPH J. BARYCKI,[1] LAURIE K. O'BRIEN,[2] JENS J. BIRKTOFT,[3]
ARNOLD W. STRAUSS,[2] AND LEONARD J. BANASZAK[1]

[1]Department of Biochemistry, Molecular Biology, and Biophysics, University of Minnesota, Minneapolis, Minnesota 55455
[2]Department of Pediatrics, Washington University, School of Medicine, St. Louis, Missouri 63110
[3]X-taldesigns, Box 20620, New York, New York 10025

(RECEIVED April 20, 1999; ACCEPTED July 16, 1999)

Abstract

Short chain L-3-hydroxyacyl CoA dehydrogenase (SCHAD) is a soluble dimeric enzyme critical for oxidative metabolism of fatty acids. Its primary sequence has been reported to be conserved across numerous tissues and species with the notable exception of the pig heart homologue. Preliminary efforts to solve the crystal structure of the dimeric pig heart SCHAD suggested the unprecedented occurrence of three enzyme subunits within the asymmetric unit, a phenomenon that was thought to have hampered refinement of the initial chain tracing. The recently solved crystal coordinates of human heart SCHAD facilitated a molecular replacement solution to the pig heart SCHAD data. Refinement of the model, in conjunction with the nucleotide sequence for pig heart SCHAD determined in this paper, has demonstrated that the previously published pig heart SCHAD sequence was incorrect. Presented here are the corrected amino acid sequence and the high resolution crystal structure determined for pig heart SCHAD complexed with its NAD^+ cofactor (2.8 Å; R_{cryst} = 22.4%, R_{free} = 28.8%). In addition, the peculiar phenomenon of a dimeric enzyme crystallizing with three subunits contained in the asymmetric unit is described.

Keywords: β-oxidation; dehydrogenase; primary sequence; SCHAD; X-ray structure

During the metabolism of fatty acids by the β-oxidation spiral, L-3-hydroxyacyl-CoA dehydrogenase [EC 1.1.1.35] catalyzes the oxidation of the hydroxyl group of L-3-hydroxyacyl-CoA to a keto group, concomitant with the reduction of NAD^+ to NADH, as shown in Scheme 1. The enzyme is a "B-side"-specific dehydrogenase (Noyes et al., 1974) with hydride transfer occurring on the *si* face of the nicotinamide ring. An active site His-Glu pair is thought to be essential for catalysis with histidine serving as a general base in the abstraction of the proton from the 3-hydroxyl group of the substrate. The conserved glutamate has been shown to position the active site histidine and may modulate its pK_a (He & Yang, 1996; Barycki et al., 1999).

Two forms of L-3-hydroxyacyl-CoA dehydrogenase are generally encountered. Short chain L-3-hydroxyacyl-CoA dehydrogenase (SCHAD) is a soluble dimeric enzyme with a subunit molecular weight of ~34 kDa. It demonstrates fairly broad substrate specificity using substrates containing 4–16 carbons in the acyl chain, but exhibits significant product inhibition with longer chain substrates (Kobayashi et al., 1996). Long chain L-3-hydroxyacyl-CoA dehydrogenase (LCHAD) is a component of a membrane-associated multifunctional enzyme complex and displays optimal activity toward substrates with 12–16 carbons in the acyl chain. SCHAD and LCHAD share considerable sequence homology and display overlapping substrate specificity (Schulz, 1996). A third enzyme, which also catalyzes the oxidation of short chain L-3-hydroxyacyl-CoA substrates, has been reported, but it is probably not a member of this enzyme family since it shares no

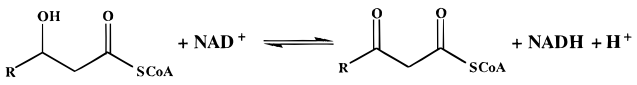

Scheme 1.

Reprint requests to: Dr. Leonard J. Banaszak, Dietrich Professor of Biochemistry, Department of Biochemistry, Molecular Biology, and Biophysics, 4-225 Millard Hall, 435 Delaware Street S.E., Minneapolis, Minnesota 55455; e-mail: len_b@dcmir.med.umn.edu.

Abbreviations: AFLP, acute fatty liver of pregnancy; CNS, Crystallography and NMR System; DTT, dithiothreitol; FOM, figure of merit; LCHAD, long chain L-3-hydroxyacyl CoA dehydrogenase; RMSD, root-mean-square deviation; RT-PCR, reverse transcription followed by polymerase chain reaction; SCHAD, short chain L-3-hydroxyacyl CoA dehydrogenase.

significant sequence homology to SCHAD or LCHAD (Furuta et al., 1997).

Clinically, deficiencies of SCHAD and LCHAD activities are manifested as hypoketotic hypoglycemia, hypertrophic cardiomyopathy, skeletal myopathy, and liver dysfunction (Bennett et al., 1996; Isaacs et al., 1996; Pons et al., 1996). One of the most common mutations resulting in LCHAD deficiency is the substitution of the active site glutamate with a glutamine residue (E474Q) within the α-subunit of human mitochondrial trifunctional protein. This mutation within the His-Glu active site pair has been correlated with maternal acute fatty liver of pregnancy (AFLP), sudden unexplained infant death, and Reye-like syndrome (Isaacs et al., 1996). Because LCHAD is a component of a membrane associated multienzyme complex, its characterization is inherently more complex. Therefore, most studies have focused on the soluble dimeric SCHAD and its properties.

An examination of a previous amino acid sequence alignment of multiple L-3-hydroxyacyl-CoA dehydrogenases (Barycki et al., 1999) suggested that pig heart SCHAD may be of biochemical interest due to unique regions within its primary sequence. In particular, a two amino acid deletion and a seven amino acid insertion had been reported for the pig heart enzyme (Bitar et al., 1980), neither of which are observed within the numerous LCHAD and SCHAD sequences examined. The two amino acid deletion occurred after Phe159, in the region between the active site histidine, His158, and the required glutamate residue, Glu170. The seven amino acid insertion was found after Glu110 in the NAD^+ binding domain. As judged by comparison with the human heart SCHAD crystal structure (Barycki et al., 1999), the insertion would occur in a region involved in coordination of the nicotinamide ribose ring. Recently, the cloning and sequencing of pig liver SCHAD were reported (He & Yang, 1998). The pig liver enzyme sequence also differs from that previously reported for pig heart in the same key regions. The authors cite different catalytic properties for the pig liver enzyme relative to the pig heart enzyme, which along with the sequence differences, suggest the existence of different isoforms of SCHAD. However, the primary sequence and structural determinations reported in this paper call these assertions into question.

In addition to its potential biochemical interest, the structure determination of pig heart SCHAD provided a chance to study an intriguing crystallographic phenomenon. A preliminary α-carbon chain tracing of pig heart SCHAD complexed with NAD^+ was described in a previous report from this laboratory (Birktoft et al., 1987). However, the pig heart model could not be sufficiently refined to include amino acid side-chain positions presumably because of the peculiar occurrence of 1.5 dimers (i.e., three subunits) within the asymmetric unit. Assisted by the recently solved human heart structure, this unique crystallographic occurrence has been re-examined in an effort to gain insight into the supposed tissue-specific differences among pig L-3-hydroxyacyl-CoA dehydrogenases. The original pig heart SCHAD diffraction data were evaluated using molecular replacement techniques and the cDNA sequence determined. The structural model for pig heart L-3-hydroxyacyl-CoA dehydrogenase[4] was found to be consistent with the deduced amino acid sequence, both of which confirm the identity of pig heart and liver SCHAD, and illustrates an intriguing crystal packing phenomenon.

[4]Coordinates and structure factors for pig heart SCHAD have been deposited in the Protein Data Bank (PDB) with accession codes 3hdh and r3hdhsf, respectively.

Results

Molecular replacement and model building

Molecular replacement techniques using the dimeric human heart SCHAD structure as a probe provided an unambiguous solution to the phase problem of the pig heart diffraction data set. Three of the top five possible molecular replacement solutions were equivalent and the initial model placement resulted in an R_{cryst} of 43.7%. Furthermore, examination of $|F_o| - |F_c|$ electron density maps revealed well-defined density for NAD^+ bound to subunits A and B, even though coordinates for the cofactors were not included in the probe. Similarly, as noted below, density was observed for the third subunit, subunit C. These observations indicate that the correct molecular replacement solution was selected. After the initial rounds of refinement, two facts became readily apparent. First, the previously published amino acid sequence of pig heart SCHAD is incorrect. Second, three subunits are indeed contained within the asymmetric unit as previously reported. The first point is best illustrated by the electron density shown in Figure 1. Depicted are residues 105–119 of subunit A of the final pig heart SCHAD model superimposed on a $2|F_o| - |F_c|$ simulated annealing omit map of the region, contoured at 1σ. The previously reported pig heart sequence predicted a seven amino acid insert between residues Glu110 and Asn111. No density for this insert was observed, and the existing density corresponded closely to the human heart SCHAD model. Similarly, a two amino acid deletion after Phe159, as predicted by the previous report, is not evident. The density in this region also correlated with the human heart model and was confirmed in a simulated annealing omit map (data not shown). Therefore, the density was modeled using the sequence of the human heart enzyme until that of the pig heart could be determined (see below). Refinement of the complete dimer contained in the asymmetric unit, the A-B dimer, proceeded without incident.

The presence of a third subunit within the asymmetric unit had been suggested in previous studies (Holden & Banaszak, 1983; Birktoft et al., 1987). However, the unique packing arrangement had been viewed with some skepticism considering the enzyme is active as a dimer, and the refinement could not progress beyond a preliminary α-carbon tracing. In this paper, several secondary structure elements of the third subunit were visible within the electron density after initial placement of the search probe. Within a few rounds of refinement (R_{cryst} = 31.8%, R_{free} = 38.2%), the third subunit could be partially seen along the crystallographic twofold axis (Fig. 2). The coordinates for subunit A were then used to begin modeling the third subunit; subunit C was initially placed by visually aligning the secondary structure elements of the NAD^+ binding domain into the electron density. Many side chains were clearly identified in this region, which aided in the initial placement. Note that since the human heart SCHAD dimer was used as the probe, the presence of the C-subunit was not detected in the molecular replacement solutions. Rigid body refinement of the third subunit yielded a model with R_{cryst} = 28.8% and R_{free} = 32.6%.

Examination of the map in the region of subunit C revealed that the electron density was considerably weaker for the third subunit compared to the other subunits. In particular, the C-terminal domain of subunit C appeared quite disordered, although weak den-

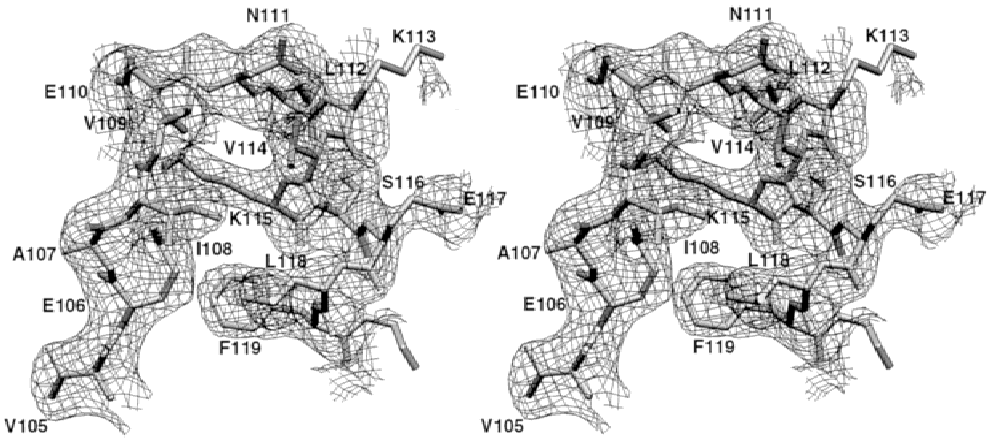

Fig. 1. Stereodiagram of a simulated annealing $2|F_o| - |F_c|$ omit map contoured at 1σ. The electron density corresponds to the region of the proposed seven amino acid insertion between residues Glu110 and Asn111. Also shown for comparison are residues 105–119 of the final pig heart SCHAD model.

sity could be observed for several of its α-helices. Furthermore, *B*-factor refinement of the three subunits as individual domains suggested that the average *B*-factor for subunit C was more than 40 Å^2 greater than subunit A. Evaluation of the model of subunit C also suggested some problem with its placement. Generation of the symmetry mate of subunit C to produce the C–C dimer indicated subunit–subunit interactions quite different than those observed in the A–B dimer. In fact, numerous steric overlaps were observed across the crystallographic twofold axis. The loop regions in the C-terminal domain were removed, and the α-helical regions of the C-terminal domain were then subjected to rigid body refinement. The resulting electron density map allowed several of the loop regions in the C-terminal domain to be rebuilt. Empirical calculations that monitored R_{cryst} and R_{free} suggested that residues 245–254 and 278–295 of subunit C be assigned occupancies of 0.5 to reflect their relative disorder. Despite attempts to improve the density in this region, numerous $|F_o| - |F_c|$ peaks are observed in the C-terminal domain of subunit C in the final model. The density in the NAD^+ binding domain is reasonably well defined, but the *B*-factors of atoms in this region are quite high (>80 Å^2). Although the presence of the third subunit within the asymmetric unit is evident, the model in this region should be viewed with suspicion due to the considerable disorder that has been observed.

Statistics for the final SCHAD model, which has an R_{cryst} = 22.4% and R_{free} = 28.8%, are given in Table 1. Three amino acid residues are found in the "disallowed" region of the Ramachandran plot as judged by analysis with PROCHECK (Laskowski et al., 1993). They correspond to Phe205 of each subunit and adopt a

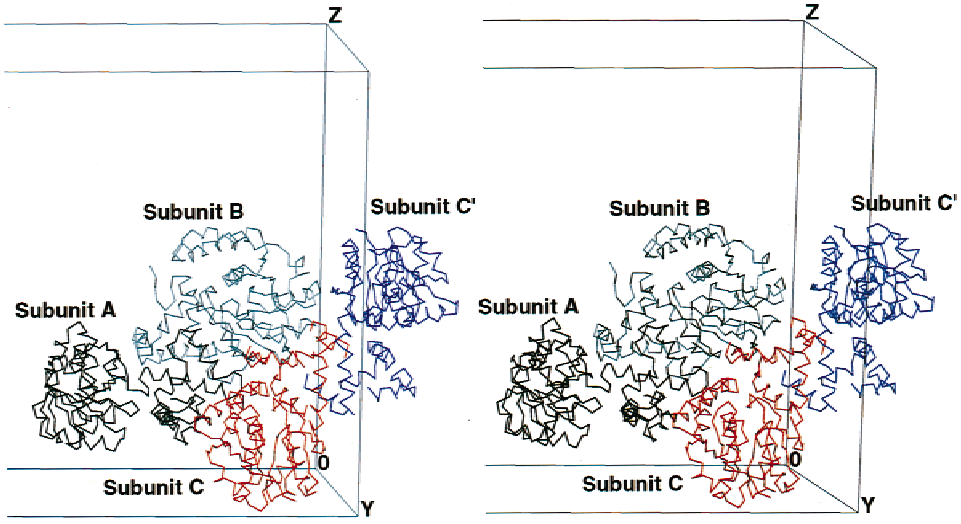

Fig. 2. Stereodiagram of a section of the pig heart SCHAD unit cell. The unusual occurrence of three subunits within the asymmetric unit is illustrated in relation to the crystallographic symmetry axis. Subunits A and B (black and gray, respectively) form a dimer related by local symmetry within the asymmetric unit. However, the oligomerization interface of subunit C (red) and its dimeric partner C′ (blue) is coincident with a crystallographic twofold rotation axis.

Table 1. *Model and refinement statistics of pig heart SCHAD*

Resolution	20–2.8 Å
σ cutoff	1.0
Number of reflections	24,618
Completeness (highest shell)	84.7% (63.2%)
R_{cryst} (highest shell)[a]	22.4% (31.6%)
R_{free} (highest shell)[b]	28.8% (34.4%)
Number of protein atoms	6510
Number of ligand atoms	132
Number of water molecules	23
Average *B*-factor	
Subunit A	48.2 Å
Subunit B	57.6 Å
Subunit C	82.1 Å
RMSD bond lengths	0.009 Å
RMSD bond angles	1.50°
RMSD dihedral	21.1°
RMSD improper	0.80°
Ramachandran geometry[c]	
Most favored	81.7%
Allowed	17.7%
Generously allowed	0.3%
Disallowed	0.4%
cis-Peptides	3

[a] $R_{cryst} = \sum|F_o - F_c|/\sum|F_o|$.
[b] An R_{free} test set of 5% of the total reflections was used.
[c] The Ramachandran geometry was monitored using PROCHECK (Laskowski et al., 1993).

conformation near the β-turn region of the Ramachandran plot. This unusual geometry is stabilized by numerous electrostatic interactions, several of which are also involved in positioning the active site glutamate, E170. As mentioned above, the average *B*-factor for subunit C is considerably higher than that of either subunit A or B, which reflects the relative disorder of this subunit. Overall, the statistics are comparable to those of other structures determined at this resolution.

Sequence determinations of pig heart and pig smooth muscle SCHAD

Discrepancies between the observed electron density and the previously published pig heart SCHAD primary structure prompted the re-examination of the sequence information. The pig heart sequence had been determined by Edman degradation of proteolytic peptide fragments (Bitar et al., 1980). In the current study, total pig heart RNA was subjected to RT-PCR using SCHAD specific oligomers and the resultant single product sequenced as described in Materials and methods. The deduced amino acid sequence of pig heart SCHAD determined by this method is presented in Figure 3. Probing a pig smooth muscle cDNA library (Stratagene, La Jolla, California) with human heart SCHAD cDNA revealed a single gene product, which was also sequenced and is shown for comparison, as are the previously determined pig heart, pig liver, and human heart SCHAD sequences (Fig. 3). The newly determined pig heart and the pig smooth muscle sequences are virtually identical at the nucleotide level with only a silent single base substitution difference (data not shown). They do not contain either the seven amino acid insert after Glu110 or the two amino acid deletion after Phe159 as reported previously (Bitar et al., 1980). Furthermore, the pig heart amino acid sequence is identical to the liver sequence as deposited in Genbank (AF027652). This strong conservation of primary structure continues across species with the pig heart exhibiting nearly 95% identity to the human heart sequence.

Overall structure

Once the corrected pig heart SCHAD sequence became available, model refinements were completed. The pig heart SCHAD monomer is depicted in Figure 4 with the N- and C-termini labeled and the NAD^+ cofactor indicated. Briefly, SCHAD exhibits a two domain topology with the N-terminal domain (residues 12–201) of each subunit containing an eight-stranded β-sheet. The first six β-strands are parallel and adopt a typical Rossmann fold that accommodates binding of NAD^+. The remaining two strands are also parallel but in the opposite direction of the first six. The active site residues His158 and Glu170 are located in strands β6 and β7, respectively. The C-terminal domain (residues 207–302) of each monomer is primarily alpha helical and mediates subunit–subunit dimerization. The orientation of the NAD^+-binding domain relative to the C-terminal domain is determined by a short linker region (residues 202–206), which appears to be important in correct positioning of putative active site residues. The pig heart structure is nearly identical to the equivalent human structure with a RMS deviation (RMSD) of 0.96 Å for α-carbons. This is comparable to the variations observed between subunits of the pig heart crystal structure. For example, subunits A and B exhibit an RMSD of 0.92 Å. Therefore, the reader is referred to the description of the human heart enzyme, which was determined at 2.0 Å resolution, for further details of the tertiary structure (Barycki et al., 1999).

One of only two significant differences between the human and pig heart structures occurs within the helix-turn-helix motif (α2,α3) of subunit B (Fig. 5). Between residues 60B through 80B, an RMSD of 3.3 Å for α-carbons is observed. The inward bend of the helix-turn-helix "tail" in the pig heart structure is the result of steric repulsion. Specifically, if residues 71–75 of subunit B were to remain in a conformation similar to the corresponding human structure, they would overlap residues Asp93, Ser96, His99, and Phe125 of the symmetry-related subunit A. As the pig heart structure is modeled, the closest contact between the "tail" of subunit B and the symmetry-related subunit A is greater than 3 Å and occurs between the backbone carbonyl of Glu72B and the aromatic ring of Phe125A.

The other significant difference is found at the interface of the C–C dimer. The interactions observed for the formation of the human heart SCHAD dimer and the A–B dimer of the pig heart enzyme structure are not present in the C–C dimer. Overall, the A–B dimer exhibits an RMSD of 2.6 Å with respect to the C–C dimer. The relatively high deviation is primarily the result of a shift at the C–C dimer interface of ~3 Å. In particular, the previously described Arg209–Glu117 salt bridges as well as the Asp231–Ser198 and Lys200–Asp226 hydrogen bond pairs have been disrupted. They have been replaced by salt bridges between the side chains of Arg220 and Glu217 of opposing subunits. However, it is important to note that the density in this region is quite weak and may not reflect a true dimer interface. In fact, removal of the entire C-terminal domain of the C-subunit results in only a 0.7% increase in R_{free}.

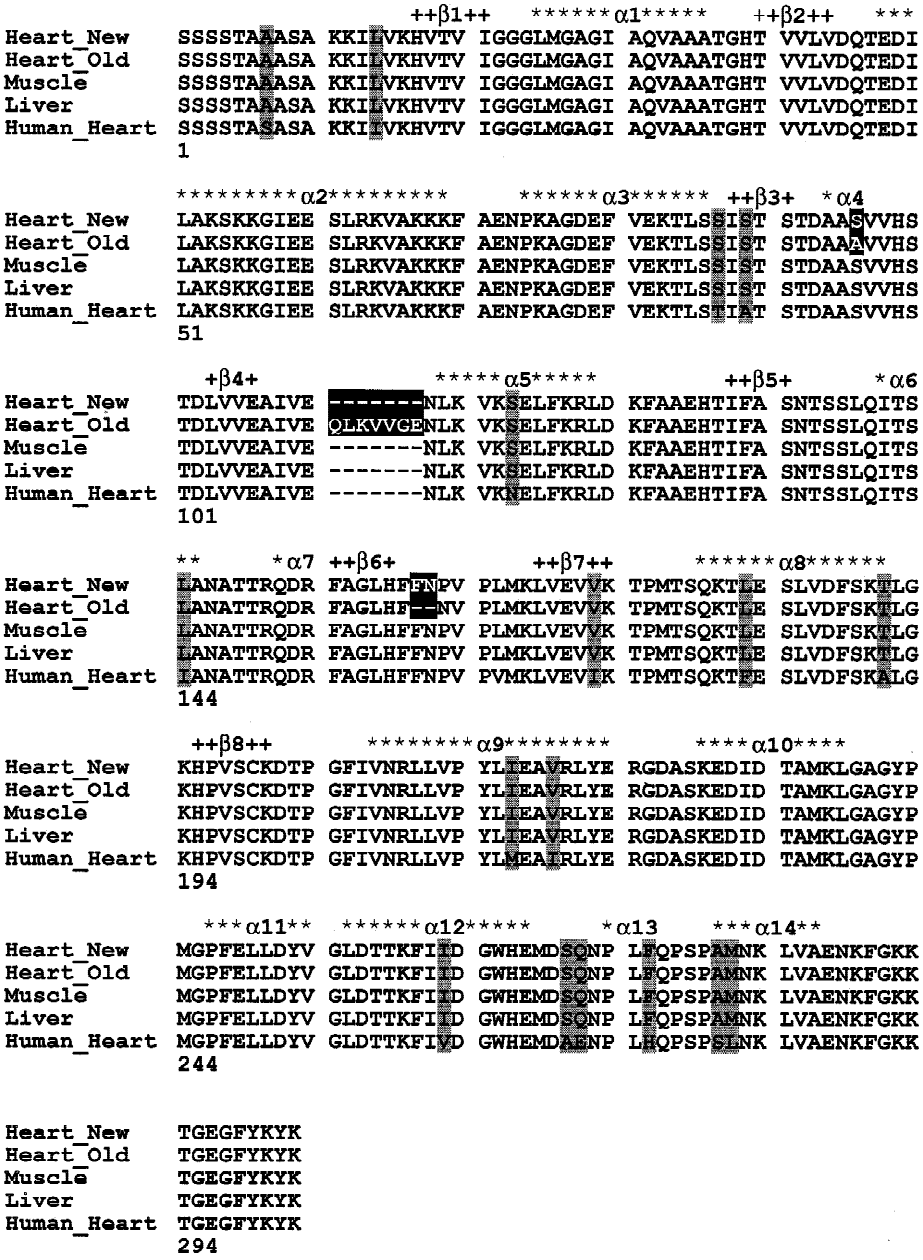

Fig. 3. Sequence alignment of several L-3-hydroxyacyl CoA dehydrogenases. Sequence errors between the previously reported pig heart SCHAD sequence (Heart_Old) and the current pig heart sequence (Heart_New) are highlighted in black. Also shown for comparison are the pig smooth muscle SCHAD sequence (Muscle), the pig liver SCHAD sequence (Liver), and the human heart primary structure (Human_Heart), with conservatively substituted residues shown in grey. Uncolored residues are identical among all sequences. Amino acids are numbered according to the current pig heart sequence with corresponding secondary structure elements of the pig heart model indicated.

Discussion

The amino acid sequence and three-dimensional structure of pig heart SCHAD have been re-evaluated as a result of recent advances in the study of L-3-hydroxyacyl-CoA dehydrogenases. Crystallographic data obtained from pig heart SCHAD nearly 15 years ago have been re-interpreted using the human heart SCHAD crystal structure as a molecular replacement probe. The structure of pig heart SCHAD has been determined and confirms previous indications that three subunits are indeed contained in the asymmetric unit (Holden & Banaszak, 1983). This is particularly interesting considering the enzyme is biologically active as a dimer. Two subunits occur as a dimer within the asymmetric unit using local symmetry. The required twofold symmetry of the third subunit, however, is coincident with the crystallographic twofold axis. The overall fold of pig heart SCHAD is comparable to a previously reported preliminary chain tracing (Birktoft et al., 1987), as well as to the analogous human enzyme structure. The pig heart structure

Fig. 4. Pig heart SCHAD model. A single subunit of pig heart SCHAD is modeled as a ribbon diagram. Secondary structure elements are labeled and numbered sequentially from N to C terminus as in Figure 3. The NAD^+ cofactor, rendered as a ball and stick model, is also indicated.

contains an NAD^+ binding domain that adopts a typical nucleotide-binding fold and a C-terminal domain, which is primarily α-helical and mediates subunit dimerization. The cDNAs for pig heart and pig smooth muscle SCHAD have been subcloned and sequenced. The deduced amino acid sequences were compared to a previously reported pig heart SCHAD amino acid sequence and to the recently described pig liver SCHAD primary sequence. Amino acid identity between pig liver, smooth muscle, and the newly determined heart sequence indicates errors in the pig heart SCHAD sequence described previously (Bitar et al., 1980).

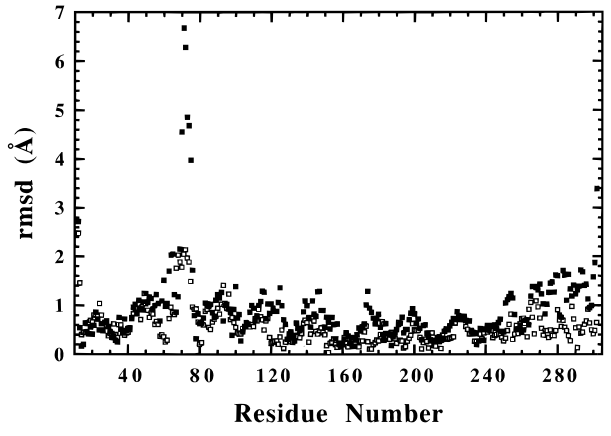

Fig. 5. Similarity of pig and human heart SCHAD subunit models. RMSDs were calculated for each residue of human vs. pig SCHAD subunit A (open symbols) and subunit B (filled symbols). Results are plotted as RMSD vs. residue number to illustrate the extremely small differences in residue position exhibited between pig and human enzyme. However, residues 60–80, corresponding to the helix-turn-helix tail, exhibit significant differences between the two models and may indicate structural flexibility.

Possible errors in the previously reported pig heart SCHAD sequence first became apparent during the initial rounds of refinement of the model. In particular, the seven amino acid insert after Glu110 was not indicated in the electron density (Fig. 1), nor was there evidence for a two amino acid deletion after Phe159. Determination of the correct pig heart primary structure confirmed that an earlier sequence determination (Bitar et al., 1980) contained minor errors. As mentioned above, the previously reported pig heart sequence was the only one with either the seven residue insert or the two amino acid deletion (Fig. 3). The initial pig heart SCHAD sequence (Bitar et al., 1980) was determined by protein chemistry techniques. The enzyme was processed into short peptides that were separated and then sequenced by Edman degradation. The individual peptide sequences were then pieced together to give the complete protein sequence. The reported deletion after Phe159 may be explained by the repetitive nature of the region. The correct sequence is His158-Phe-Phe-Asn-Pro-Val-Pro-Leu165 whereas the previous sequence reported is His-Phe-Asn-Val-Pro-Leu. Perhaps the repetitive Phe-Phe sequence was interpreted as carryover from the previous sequencing cycle. The insertion after Glu110 is harder to rationalize without the primary data. It is important to note that two protein bands were often observed by SDS-PAGE of pig heart SCHAD enzyme preparations (Bitar et al., 1980). Therefore, the possibility cannot be ruled that out that two isoforms do exist in heart tissue, and the sequence reported here describes only the species that crystallized.

Determination of the pig heart and pig smooth muscle amino acid sequences reveals that the two enzymes are identical. In light of this observation, it is unlikely that significant isoforms of the enzyme exist, particularly since a comparison of the correct pig liver and heart SCHAD sequences indicates that they too are identical (Fig. 3). Absence of SCHAD isoforms is also consistent with mouse studies in which high sequence conservation is maintained across tissues (O'Brien & Strauss, unpubl. obs.). Studies in which the catalytic activities of the heart and liver enzymes are compared directly are unlikely to demonstrate the measurable differences that had been previously reported (He & Yang, 1998).

During preparation of this paper, an independent determination of the pig heart SCHAD sequence was reported that indicated that the pig liver and pig heart SCHAD sequences are identical (He et al., 1999). Initially, we interpreted this finding in light of the published pig liver sequence (He & Yang, 1998). There are four amino acid differences between the reported liver sequence (He & Yang, 1998) and the pig heart sequence detailed here; specifically Ala7 of the pig heart sequence was reported as Ser in liver, Ile50 as Thr, Ala66 as Val, and Ser116 as Asn. These substitutions were suggestive of polymorphisms between heart tissue samples. However, a closer examination of the pig heart sequence report (He et al., 1999) reveals an ambiguity within the literature. In particular, the SCHAD sequence reported (He et al., 1999) is identical to the pig heart sequence determined here. Therefore, it is likely that the reported pig liver sequence (He & Yang, 1998) is inaccurate. Furthermore, the sequences for both enzymes have been deposited in Genbank and are identical. The correct primary structures of pig heart, liver, and smooth muscle SCHAD are aligned in Figure 3.

A comparison of the final pig heart SCHAD model (A–B dimer) and the human heart enzyme structure reveals that the two are nearly identical (Fig. 5). This similarity is expected considering their strong sequence homology (Fig. 3). For α-carbons, the two models have an RMSD of 0.96 Å; this value drops to 0.76 Å when

residues 60B through 80B, corresponding to the helix-turn-helix "tail" of subunit B, are omitted from the calculation. The two α-helices that extend from the NAD^+ binding domain of subunit B in the pig heart structure are considerably shifted with respect to the corresponding region of the human structure. This observation is consistent with the relatively high *B*-factors observed in this region, which suggest a high degree of mobility.

A function for the helix-turn-helix "tail," which connects strands β2 and β3 of the NAD^+-binding domain, has yet to be ascribed. This motif contains numerous polar residues (Fig. 3) and extends from the globular NAD^+ binding domain (Fig. 4). A sequence comparison of several L-3-hydroxyacyl CoA dehydrogenases does not indicate strict conservation of amino acid residues in this region, but an abundance of polar residues is clearly observed (Barycki et al., 1999). The "tail" may serve as a contact site for undefined electrostatic intermolecular interactions through its charged amino acid side chains. The high mobility observed in this region may facilitate such an interaction. An attractive candidate for binding at this site is the adenylate component of the acyl-CoA substrate. The charged phosphate groups of this moiety have been predicted by spin-labeling and molecular modeling studies to be in the vicinity of the helix-turn-helix tail (Hartmann et al., 1991). Alternatively, this motif may be a vestige of a prior functional domain. A similar protrusion is observed in the structurally homologous FAD binding domain of glutathione reductase (Mittl & Schulz, 1994). Subunit oligomerization is mediated through this appendage in glutathione reductase, but clearly not in SCHAD. Perhaps the highly flexible nature of the helix-turn-helix tail in SCHAD simply reflects lack of functional importance.

The completion of the pig heart SCHAD structure also validates two points of the human heart SCHAD structural model (Barycki et al., 1999). The human heart SCHAD was expressed with an additional six-histidine arm on its C-terminal to facilitate purification. Although this recombinant enzyme displayed catalytic characteristics similar to other L-3-hydroxyacyl CoA dehydrogenases, the secondary structure of the enzyme could have been altered by the presence of the histidine arm. The similarity observed in the C-terminal regions of the pig and human heart structures (Fig. 5, residues 280–302) argues that the additional histidine residues are not a significant perturbation. Second, a spurious mutation was found in the human heart SCHAD cDNA, altering a phenylalanine to a cysteine residue (F80C). This substitution is not located at the enzyme active site and did not appear to affect enzyme structure or function. The pig heart structure, which contains a phenylalanine at position 80, justifies the human heart SCHAD model; no significant structural changes between the pig and human heart models can be attributed to the F80C substitution (Fig. 5).

A crystal packing arrangement in which three subunits were contained in the asymmetric unit for a dimeric protein was thought to be unique at the time of publication of the pig heart SCHAD α-carbon tracing. An analogous case in which three subunits are contained within the asymmetric unit for a tetrameric enzyme has recently been reported (Guenther et al., 1999). It certainly is a curious situation for identical dimeric proteins, as judged by amino acid sequence, to manifest their twofold symmetries using both local and crystallographic axes within the same crystal. Surprisingly, the third subunit exhibits the weakest density. Intuitively, one might expect that the subunit along the crystallographic twofold axis would have the strongest density; the electron density of the biological dimer would be averaged across the twofold axis and result in stronger electron density for the subunit. Clearly, this is not the case. Since the NAD^+ binding domain is relatively well defined in the third subunit, particularly at contact sites with the A–B dimer, the poor density observed may be the result of disorder in the C-terminal domain. The orientation of the C-terminal domain relative to the NAD^+ binding domain is determined by a short linker region (residues 202–206) that contains the highly conserved PGF sequence (Fig. 3). Perhaps this region serves as a hinge between the two domains and thus allows a considerable range of motion.

Previous attempts to complete the pig heart SCHAD model were certainly hampered by having both a partially incorrect amino acid sequence and a peculiar occurrence of three subunits within the asymmetric unit. The unusual crystal packing by itself should not have precluded a successful structure determination as evidenced here. Furthermore, the errors in the amino acid sequence should have presented themselves had the initial phase information been more accurate. Unfortunately, the initial electron density maps were of marginal quality extending only to 3 Å. Thus, the ambiguities introduced by sequence errors and unusual crystal packing did not allow for significant improvements to the phase information. Although the sequence errors were local in nature, they were propagated along the peptide backbone once initial amino acid assignments were made. Without significant improvements in the A–B dimer due to incorrect amino acid placements, the density for the C-subunit remained nebulous. Even with good starting phase information obtained via molecular replacement, clear density for the NAD^+ binding domain of subunit C was not observed until later rounds of refinement as indicated in Results. Remarkably, the overall fold of the previously reported preliminary chain tracing of pig heart SCHAD (Birktoft et al., 1987) is comparable to the model described here, indicating that the initial phase information obtained by multiple isomorphous replacement techniques was valid.

In summary, the primary amino acid sequence and high resolution crystal structure of pig heart SCHAD have been determined. The completion of the pig heart SCHAD model was facilitated by the use of the independently determined human heart SCHAD structure as a molecular replacement probe. Examination of the electron density maps identified possible sequence errors within the previously reported pig heart enzyme sequence and validated the presence of 1.5 dimers in the asymmetric unit. The pig heart model and primary sequence determined are both nearly identical to those of the homologous human enzyme.

Materials and methods

Purification, crystallization, and X-ray diffraction studies of SCHAD

The diffraction data used for the current study were obtained as described previously (Birktoft et al., 1987). Briefly, SCHAD was purified from pig heart tissue using ammonium sulfate precipitation, gel filtration, and ion exchange chromatography (Noyes & Bradshaw, 1973). Crystals were grown in 10 mM Tris, pH 8.0, containing 1 mM dithiothreitol (DTT) and 0.05% NaN_3, at room temperature using a protein concentration of 5 mg/mL. Typically, crystals were obtained within the precipitant range of 11 to 14% polyethylene glycol 6000 (w/v). They belong to the space group $C222_1$, with unit cell dimensions of $a = 227.2$ Å, $b = 82.2$ Å, and $c = 124.7$ Å. Crystal density measurements suggested the unusual occurrence of three subunits within the asymmetric unit, despite the fact that the enzyme is active as a dimer. A noncrystallographic

symmetry axis was also detected at polar angles of $\phi = 45°$, $\psi = 45°$, and $\kappa = 180°$ (Holden & Banaszak, 1983). Diffraction data were collected at the University of California at San Diego and extended to 2.8 Å resolution. The data set obtained from crystals of SCHAD complexed with NAD^+ was greater than 98% complete (85% in the outer most shell) with an $R_{merge} = 4.6\%$ (Birktoft et al., 1987).

Structure determination

The structure of pig heart SCHAD was determined by molecular replacement techniques using the Crystallography and NMR System (CNS) software package (Brünger et al., 1998). The dimeric model of human heart SCHAD (Barycki et al., 1999) was used as a probe, and data from 15 to 4 Å were evaluated. The initial cross rotation search provided five possible solutions. Subsequent Patterson correlation refinement followed by a translation search using each possible cross-rotation solution yielded an unambiguous solution, with three of the initial self-rotation solutions giving nearly identical results. The initial R_{cryst} was 43.7%, which dropped to 41.9% after rigid body refinement. The resulting phase information produced a readily interpretable electron density map.

Model building and refinement

The model was refined using CNS (Brünger et al., 1998), with a bulk solvent correction and a refinement target of "maximum likelihood based on amplitudes" employed throughout refinement; noncrystallographic symmetry constraints were not used. The initial rounds of model refinement included torsional dynamics, simulated annealing, positional refinement, and *B*-factor refinement, with simulated annealing omitted in later refinement rounds. The program O (Jones et al., 1991) was used to substitute residues of the human heart structure with those corresponding to the pig heart sequence and for model rebuilding after each round of refinement. Ambiguous regions of the electron density map were evaluated using $2|F_o| - |F_c|$ simulated annealing omit maps, in which designated regions of the structure were omitted and the remaining model subjected to simulated annealing prior to map calculation. Water molecules obeying proper hydrogen-bonding constraints with electron densities greater than 1.0σ on a $2|F_o| - |F_c|$ map and 4.0σ on an $|F_o| - |F_c|$ map, and the cofactor NAD^+ were also included as the model neared completion. The coordinates for NAD^+ were obtained from the Heterocompound Information Centre (Uppsala, Sweden) (HIC-Up). Coordinates for the pig heart SCHAD structure have been deposited in the PDB under the accession code 3hdh.

Sequence determination of pig heart and pig smooth muscle SCHAD

To obtain the nucleotide sequence of pig heart SCHAD, total RNA was isolated from a pig heart using the RNazol B purification kit (Tel-Test, Inc., Friendswood, Texas), and the first strand of the cDNA synthesized with oligo-dT using the Ready-To-Go T-primed first-strand kit (Pharmacia Biotech, Piscataway, New Jersey). Initial PCR amplification was primed by a 5′ oligo corresponding to the human cDNA transit peptide sequence (MAFVTRQF) using oligo-dT as the downstream primer. To ensure the specificity of the initial amplified product, this reaction was used as the template for a second PCR using the same 5′ oligo in conjunction with a 3′ oligo also derived from the human sequence. Specific oligo sequences are: 5′ oligo ATGGCCTTCGTCACCAGGCAGTTC; 3′ oligo, TCACTTGTATTTGTAAAATCCTTCTCC. The second PCR yielded a single product, which was sequenced directly by dideoxy chain termination. The final eight residues of the pig heart sequence are derived from the oligos employed and not from the isolated mRNA. The cDNA for pig smooth muscle SCHAD was obtained from Stratagene's porcine smooth muscle (aorta) cDNA library, using exon 1 of the human SCHAD gene as a probe for screening. A single clone with a 1.8 kb insert was isolated, and the nucleotide sequence was determined by dideoxy chain termination.

Acknowledgments

The authors recognize Ed Hoeffner for his contributions through the maintenance of the X-ray and computational resources at the University of Minnesota, and also Axel Brünger for providing us with the beta version of CNS. We are also grateful to Dr. Melanie Simpson for thoughtful discussions regarding the manuscript. This project was supported by a NIH post-doctoral fellowship grant to J.J.B. (1F32-DK09759-01), research support to L.J.B. from the NIH (GM13925), and computational support from the Minnesota Super Computing Institute.

References

Barycki JJ, O'Brien LK, Bratt JM, Zhang R, Sanishvili R, Strauss AW, Banaszak LJ. 1999. Biochemical characterization and crystal structure determination of human heart short chain L-3-hydroxyacyl-CoA dehydrogenase provide insights into catalytic mechanism. *Biochemistry 38*:5786–5798.

Bennett MJ, Weinberger MJ, Kobori JA, Rinaldo P, Burlina AB. 1996. Mitochondrial short-chain L-3-hydroxyacyl-coenzyme A dehydrogenase deficiency: A new defect of fatty acid oxidation. *Pediatr Res 39*:185–188.

Birktoft JJ, Holden HM, Hamlin R, Xuong NH, Banaszak LJ. 1987. Structure of L-3-hydroxyacyl-coenzyme A dehydrogenase: Preliminary chain tracing at 2.8-Å resolution. *Proc Natl Acad Sci USA 84*:8262–8266.

Bitar KG, Perez-Aranda A, Bradshaw RA. 1980. Amino acid sequence of L-3-hydroxyacyl CoA dehydrogenase from pig heart muscle. *FEBS Lett 116*: 196–198.

Brünger AT, Adams PD, Clore GM, DeLano WL, Gros P, Grosse-Kunstleve RW, Jiang JS, Kuszewski J, Nilges M, Pannu NS, et al. 1998. Crystallography & NMR system: A new software suite for macromolecular structure determination. *Acta Crystallogr D Biol Crystallogr 54*:905–921.

Furuta S, Kobayashi A, Miyazawa S, Hashimoto T. 1997. Cloning and expression of cDNA for a newly identified isozyme of bovine liver 3-hydroxyacyl-CoA dehydrogenase and its import into mitochondria. *Biochim Biophys Acta 1350*:317–324.

Guenther BD, Sheppard CA, Tran P, Rozen R, Matthews RG, Ludwig ML. 1999. The structure and properties of methylenetetrahydrofolate reductase from *Escherichia coli* suggest how folate ameliorates human hyperhomocysteinemia [see Comments]. *Nature Struct Biol 6*:359–365.

Hartmann D, Philipp R, Schmadel K, Birktoft JJ, Banaszak LJ, Trommer WE. 1991. Spatial arrangement of coenzyme and substrates bound to L-3-hydroxyacyl-CoA dehydrogenase as studied by spin-labeled analogues of NAD+ and CoA. *Biochemistry 30*:2782–2790.

He XY, Yang SY. 1996. Histidine-450 is the catalytic residue of L-3-hydroxyacyl coenzyme A dehydrogenase associated with the large alpha-subunit of the multienzyme complex of fatty acid oxidation from *Escherichia coli*. *Biochemistry 35*:9625–9630.

He XY, Yang SY. 1998. Molecular cloning, expression in *Escherichia coli*, and characterization of a novel L-3-hydroxyacyl coenzyme A dehydrogenase from pig liver. *Biochim Biophys Acta 1392*:119–126.

He XY, Zhang G, Blecha F, Yang SY. 1999. Identity of heart and liver L-3-hydroxyacyl coenzyme A dehydrogenase. *Biochim Biophys Acta 1437*:119–123.

Holden HM, Banaszak LJ. 1983. L-3-hydroxyacyl coenzyme A dehydrogenase. The location of NAD binding sites and the bilobal subunit structure. *J Biol Chem 258*:2383–2389.

Isaacs JD Jr, Sims HF, Powell CK, Bennett MJ, Hale DE, Treem WR, Strauss AW. 1996. Maternal acute fatty liver of pregnancy associated with fetal trifunctional protein deficiency: Molecular characterization of a novel maternal mutant allele. *Pediatr Res 40*:393–398.

Jones TA, Zou JY, Cowan SW, Kjeldgaard. 1991. Improved methods for binding protein models in electron density maps and the location of errors in these models. *Acta Crystallogr A 47*:110–119.

Kobayashi A, Jiang LL, Hashimoto T. 1996. Two mitochondrial 3-hydroxyacyl-CoA dehydrogenases in bovine liver. *J Biochem (Tokyo) 119*:775–782.

Laskowski RA, Moss DS, Thornton JM. 1993. Main-chain bond lengths and bond angles in protein structures. *J Mol Biol 231*:1049–1067.

Mittl PR, Schulz GE. 1994. Structure of glutathione reductase from *Escherichia coli* at 1.86 Å resolution: Comparison with the enzyme from human erythrocytes. *Protein Sci 3*:799–809.

Noyes BE, Bradshaw RA. 1973. L-3-hydroxyacyl coenzyme A dehydrogenase from pig heart muscle. I. Purification and properties. *J Biol Chem 248*: 3052–3059.

Noyes BE, Glatthaar BE, Garavelli JS, Bradshaw RA. 1974. Structural and functional similarities between mitochondrial malate dehydrogenase and L-3-hydroxyacyl CoA dehydrogenase. *Proc Natl Acad Sci USA 71*:1334–1338.

Pons R, Roig M, Riudor E, Ribes A, Briones P, Ortigosa L, Baldellou A, Gil-Gibernau J, Olesti M, Navarro C, Wanders RJ. 1996. The clinical spectrum of long-chain 3-hydroxyacyl-CoA dehydrogenase deficiency. *Pediatr Neurol 14*:236–243.

Schulz H. 1996. In: Vance DE, Vance J, eds. *Biochemistry of lipids, lipoproteins and membranes*. Amsterdam: Elsevier. pp 75–99.